Study of the $Pt^{189} \rightarrow Ir^{189} \rightarrow Os^{189}$ Decay Chain*

H. R. Lewis, Jr.,† R. A. Naumann, J. M. Prospero,‡ and D. Thomas§
Palmer Physical Laboratory, Princeton University, Princeton, New Jersey
(Received July 22, 1963; revised manuscript received 12 December 1963)

Permanent magnet electron spectrographs, a double-focusing electron spectrometer, and gamma-scintillation spectrometers have been used to measure the energies and intensities of radiations which accompany the decay of Pt^{189}. From these data, the conversion coefficients, multipolarities, and mixing ratios of a number of the transitions have been determined. Some new transitions are reported, and a revised level scheme, incorporating all but one of the observed transitions, is proposed for Ir^{189}. A half-life of 10.87 ± 0.12 h has been determined for Pt^{189}. The gamma-scintillation spectrum obtained from a pure source of Ir^{189} is reported. The half-life of Ir^{189} which has been measured is 13.3 ± 0.1 days.

I. INTRODUCTION

An important problem in the study of nuclear structure is the understanding of nuclei whose properties are intermediate between those of the strongly deformed nuclei, to which the collective model applies, and those of the spherical and near-spherical nuclei, which are best described by an independent particle model. More detailed experimental knowledge about these transition nuclei is desirable for the further development and evaluation of pertinent theories: notably, the unified model,[1] and the axially asymmetric model of Davydov.[2] The neutron deficient isotopes of platinum, iridium, and osmium are of particular interest because among them can be found examples of nuclei which are in the intermediate region.

Recently, a study of the internal conversion electrons accompanying the $Pt^{189} \rightarrow Ir^{189} \rightarrow Os^{189}$ decay chain, using permanent magnet spectrographs, has been reported by Harmatz, Handley, and Mihelich.[3] Nuclear level diagrams for Ir^{189} and Os^{189}, based on energy sums and differences for the observed transitions, and on multipolarities inferred from conversion electron intensities obtained from photographic plates, have been proposed by these authors. Similar work, involving permanent magnet spectrographs, but including gamma-ray measurements and preliminary results of conversion electron measurements obtained with a double-focusing electron spectrometer, has also been reported in a thesis by one of us (JMP).[4] In addition, Lerohl[5] has made a study of the gamma radiation accompanying the decay of Ir^{189}.

In this paper we present the results of an investigation of the $Pt^{189} \rightarrow Ir^{189} \rightarrow Os^{189}$ decay chain in which the decay of these nuclides was studied by means of gamma-ray scintillation spectroscopy and conversion-electron spectroscopy, using both permanent magnet spectrographs and a double-focusing electron spectrometer.

II. SOURCE PREPARATION

Metallic iridium foils of purity greater than[6] 99.8% were irradiated with 60-MeV protons at the Nevis synchrocyclotron (Columbia University). These iridium foil targets were mounted on probes "edge-on" to the beam so that protons entered the leading edge of the foil and then traversed the $\frac{1}{4}$-in. width of the foil.

After irradiation the targets were allowed to stand for approximately ten hours, in order to permit the shorter lived isotopes of platinum to decay before chemical processing was begun. Targets were dissolved by fusion at red heat in a mixture of potassium hydroxide and potassium nitrate. After cooling, the melt was dissolved in hydrochloric acid, and the platinum was isolated by ethyl acetate extraction[7] of the platinum-tin complex from a 3 molar hydrochloric acid solution containing stannous chloride. The ethyl acetate solution was evaporated almost to dryness and the residue taken up in 6 molar hydrochloric acid containing hydrogen peroxide. After boiling, the solution was extracted three times with methyl isobutyl ketone (hexone)[8] in order to remove tetravalent tin.

The final purification of the platinum was accomplished using an ion exchange procedure.[9] The acid solution remaining after the third hexone extraction was boiled to remove hexone; the hydrochloric acid concentration was adjusted to 3 molar, and the remaining iridium then preferentially reduced by adding hydroxylamine hydrochloride to the solution and heating for 3 min in a boiling water bath. The resulting solution containing tetravalent platinum and trivalent

* This work was supported by the U. S. Atomic Energy Commission and the Higgins Scientific Trust Fund.
† Present address: Los Alamos Scientific Laboratory, P. O. Box 1663, Los Alamos, New Mexico.
‡ Present address: Marine Laboratory, Institute of Marine Science, University of Miami, Miami, Florida.
§ Present address: Foreign Office, London, England.
[1] See, for example, S. G. Nilsson, Kgl. Danske Videnskab. Selskab, Mat. Fys. Medd. **29**, No. 16 (1955); also, B. R. Mottelson and S. G. Nilsson, Kgl. Danske Videnskab. Selskab, Mat. Fys. Skrifter **1**, No. 8 (1959).
[2] See, for example, A. S. Davydov, Nucl. Phys. **16**, 597 (1960).
[3] B. Harmatz, T. H. Handley, and J. W. Mihelich, Phys. Rev. **128**, 1186 (1962).
[4] J. M. Prospero, Princeton University, Ph.D. thesis, 1962 (unpublished).
[5] J. K. Lerohl, The Ohio State University, Ph.D. thesis, 1962 (unpublished).
[6] Baker and Company, Incorporated, Newark, New Jersey.
[7] W. Wayne Meinke, University of California Radiation Laboratory Report No. UCRL-432 (unpublished).
[8] G. H. Morrison and H. Freiser, *Solvent Extraction in Analytical Chemistry* (John Wiley & Sons, Inc., New York, 1957).
[9] D. D. Busch, R. A. Naumann, and J. M. Prospero, Anal. Chem. **31**, 884 (1959).

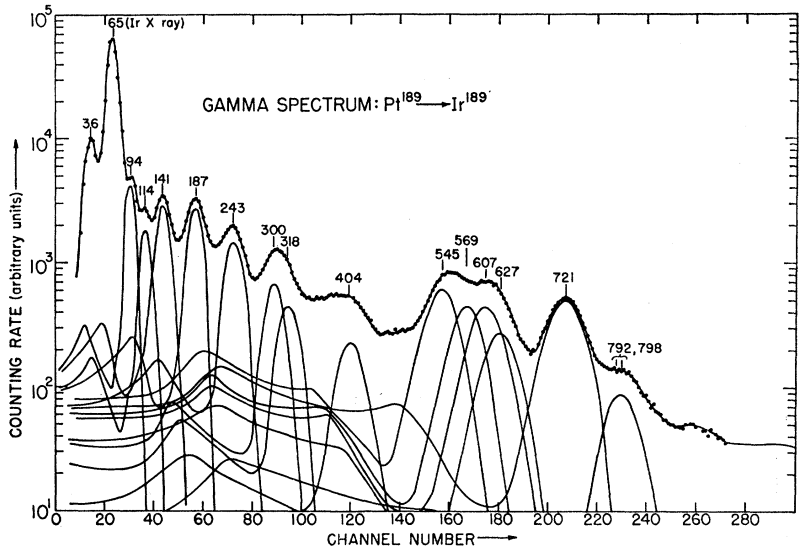

FIG. 1. Gamma spectrum of Pt^{189} showing spectral analysis.

iridium was adsorbed on a column of Dowex I anion exchange resin[10] which was maintained at 80°C by means of a water jacket. First the iridium was eluted using 9 molar hydrochloric acid; then the platinum was eluted with 50% perchloric acid.[11] The platinum-perchloric acid eluant was fumed to dryness, and the residue was then dissolved in the appropriate reagent for source preparation.

The activities observed in the platinum fraction obtained in this manner were 10-day Pt^{188}, 10.9-h Pt^{189}, 3.0-day Pt^{191} and 4.4-day Pt^{193m}. The daughter activities, Ir^{188} (41 h) and Ir^{189} (13.3 days), were observed to grow in the initially pure platinum fractions. No evidence for the presence of nuclides other than these was observed during the course of the measurements which are reported in this paper. The maximum period of measurement on a given source was approximately 2 months.

In order to obtain pure sources of Ir^{189}, an iridium separation was carried out several days after the initial platinum extraction; at the end of this time interval, essentially all of the Pt^{189} had decayed to Ir^{189}. The remaining platinum (primarily Pt^{188} and Pt^{191}) was then removed by three successive solvent extraction separations using the platinum-tin complex extraction procedure. The final purification of the iridium fraction was carried out on a Dowex I column as previously described. Because of the presence of large quantities of 41-h Ir^{188} in the iridium fraction, studies of the decay of Ir^{189} were not begun until approximately 4 weeks had elapsed from the time of purification.

Sources intended for electron spectroscopy studies were prepared by electroplating from 0.1 molar ammonium bisulfate (pH 3). Permanent magnet electron spectrograph sources were plated onto 8-mil platinum wire. Sources to be used in the double-focusing electron spectrometer were plated on one side of a 0.1-mil platinum foil; the plating area was restricted to a region approximately 1.5 mm×20 mm by means of a rubber mask. The foil or wire on which the source was plated was exposed to the full heat of a Bunsen burner before use. The active area of sources prepared in this manner was barely discernible, which testifies to their near weightlessness.

Sources for beta proportional counting and gamma spectroscopy were prepared by evaporating drops of the source solutions on $\frac{1}{4}$-mil Mylar foils supported on aluminum frames; the active deposit of each source was then covered with an additional $\frac{1}{4}$-mil Mylar foil.

A more detailed description of the chemical procedures may be found in Ref. 4.

III. GAMMA SPECTRUM STUDIES

Gamma-ray spectra were recorded using a beveled 3×3-in. NaI(Tl) scintillation detector in conjunction with a 400-channel analyzer. The detector was enclosed in a 2-in.-thick lead shield (interior dimensions 8×8 ×24 in.). The interior of this shield was covered with a copper-cadmium graded liner.

The pure platinum fraction isolated twelve hours after the termination of bombardment yielded gamma-ray spectra which maintained essentially the same characteristics for approximately 10 h. The photopeaks observed during this interval are unambiguously ascribed to radiation accompanying the decay of Pt^{189}. After this period the gamma spectrum characteristic of the Pt^{188} decay chain gradually became dominant.

A typical Pt^{189} gamma-ray spectrum is shown in Fig. 1. Gamma transitions at 94, 114, 141, 187, 243, 300, 318, 404, 545, 569, 607, 627, 721, and approximately

[10] Dow Chemical Company, Midland, Michigan. Resin Grade 200–400 mesh, 10% crosslinked. Resin column dimensions 0.3-cm diam by 1.5-cm long.

[11] All operations with perchloric acid were conducted behind explosion shields.

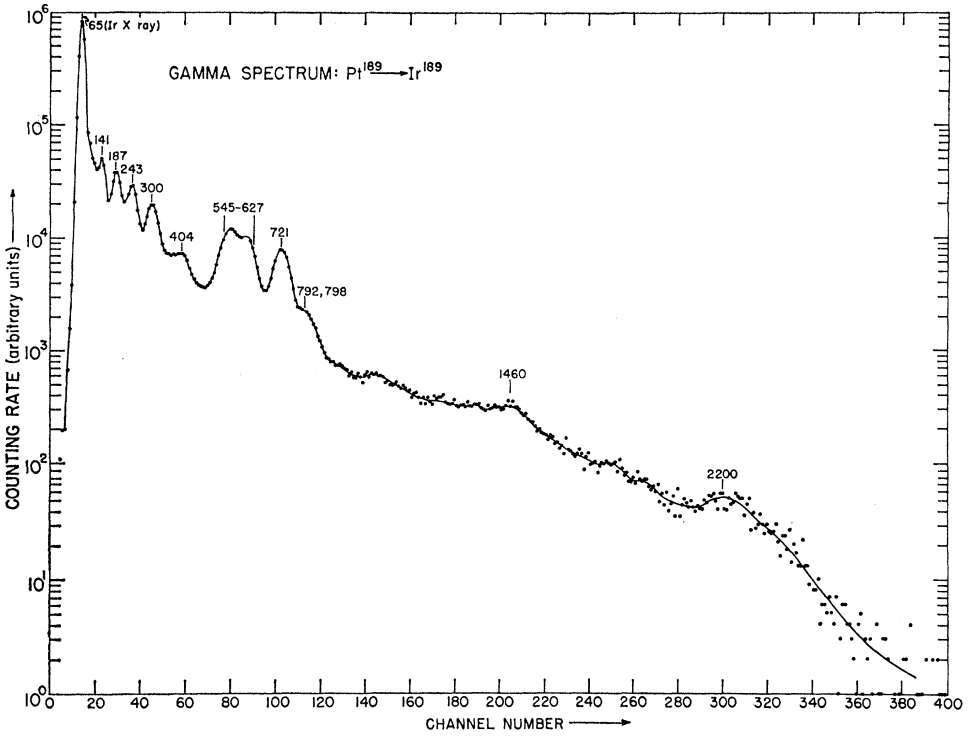

FIG. 2. Gamma spectrum of Pt^{189} recorded at reduced gain. The radiation at ~2200 keV is ascribed to the mass 188 chain.

795 keV were observed. Decomposition of this gamma spectrum was made using standard gamma ray spectra (Cs^{137}, Na^{22}, Hg^{203}, Ir^{188}) all of which were recorded using the same counting geometry; these spectra, with interpolation, yielded the individual components shown in Fig. 1. Values for the gamma ray energies represented in the composite photopeaks at 300–318 keV and 545–627 keV were obtained from the conversion electron data. Intensities for these various gamma radiations were calculated from the component photopeak areas using the published peak-to-total ratios and photopeak efficiencies of Heath.[12] These intensities are presented in Table III. The gamma spectrum of Pt^{189} recorded at reduced gain is shown in Fig. 2; it is possible that the portion of the spectrum extending from 800 keV to approximately 1.5 MeV may be due to unresolved radiations from the Pt^{189} decay. However the sharp cutoff at 2.2 MeV is characteristic of the decay of Ir^{188}. The spectra shown in Fig. 1 and Fig. 2 were recorded within 1 h after purification of the platinum fraction.

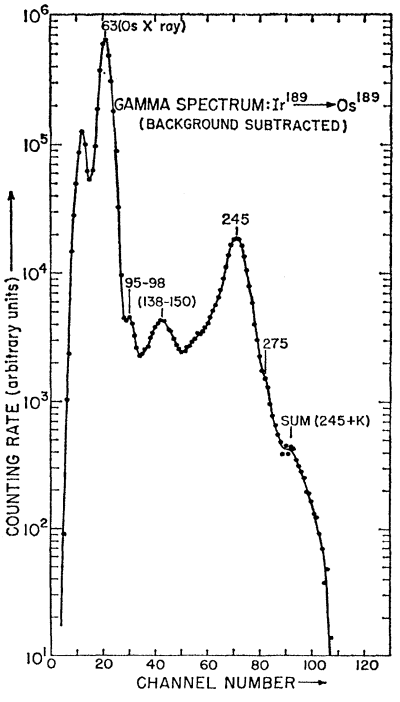

FIG. 3. Gamma spectrum of Ir^{189} recorded using a pure source.

Although detailed gamma-gamma coincidence measurements were not carried out, evidence was obtained for strong coincidence between gamma radiations in the energy interval 225–275 keV and radiations in the interval 545–570 keV. It has not been possible to satisfactorily incorporate this evidence in our decay scheme, Fig. 6.

Lerohl[5] has reported the half-life of Ir^{189} and the intensities of the gamma radiations accompanying the decay of Ir^{189}. However, these measurements were carried out with sources containing both Ir^{189} and Ir^{190}, isotopes with quite similar half-lives (13.3 days and

[12] *Scintillation Spectrometry Gamma-ray Spectrum Catalogue*, Atomic Energy Commission Report No. IDO-16408 (unpublished).

TABLE I. Intensities of the gamma transitions accompanying the decay of Pt^{189}.

Transition energy (keV)	Intensity (this work)	Intensity (Lerohl)
245	100	100
138–150	6.0	3.44
95–98	0.9	4.0
63	1314	859

12 days, respectively). It appeared worthwhile to repeat these measurements using the pure sources of Ir^{189} available from the decay of Pt^{189}. The gamma spectrum recorded with a source of pure Ir^{189} is shown in Fig. 3 and the intensities of the x radiation and composite peaks are shown in Table I, where they are compared with the values reported by Lerohl. Because of the presence of such a large number of gamma rays in so small an energy range, it was felt that a decomposition procedure was not justified.

The half-life of Ir^{189} was determined by counting Ir^{189} sources in fixed geometry using a beta proportional counter. The decay curve yields a half-life of 13.3 ± 0.1 days, in exact agreement with the value obtained by Lerohl.

IV. CONVERSION ELECTRON MEASUREMENTS

A. Instruments

Conversion electron spectra were obtained in initial experiments using three permanent magnet spectrographs. Two of the spectrographs covered the energy ranges of 5–130 keV and 10–440 keV, respectively; the third extended the coverage to 2.5 MeV. These spectra were recorded on Ilford type XM spectrographic plates which were processed with Kodak x-ray developer and replenisher and Kodak rapid fixer and hardener. The plates were read with a Norelco spectral plate reader. Only rough visual estimates of the intensities of these lines were made.

Detailed investigations of the conversion electron spectra were carried out using a $\pi\sqrt{2}$ double-focusing electron spectrometer of the Siegbahn type. The magnetic field strength near the center of this instrument was measured by means of a rotating coil system. A signal was obtained from a coil rotated in the magnetic field at 30 cycles per second by a synchronous motor; at the other end of the motor shaft, a permanent bar magnet located between a pair of Helmholtz coils was rotated at the same frequency, thereby generating a reference signal of constant amplitude in the coils. The phase difference between the rotating coil signal and the reference signal was manually adjusted to 180° by changing the orientation of the Helmholtz coils. The signal from the rotating coil and the reference signal were applied to a circuit which is schematically diagrammed in Fig. 4. The eight-position step switch and the linear 40 turn Helipot were adjusted so that the

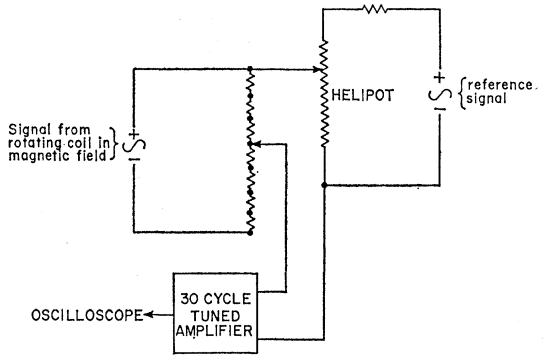

FIG. 4. Schematic diagram of the spectrometer magnetic field measuring circuit.

output of the 30 cycle/sec amplifier was a minimum, as observed on an oscilloscope. The circuit compares a fraction, f_s, of the signal from the rotating coil with a fraction, f_r, of the signal which appears across the Helipot. When the amplifier output is a minimum, the signal from the rotating coil, and therefore the magnetic field strength, is proportional to f_r/f_s. The 30-cycle/sec amplifier was very highly tuned and included rejection filters for the harmonics at 60, 90, and 120 cps. The current in the magnet coils was controlled by a slightly modified version of the constant current supply which has been described by Garwin.[13]

The electron detector used in the double-focusing spectrometer was a flow proportional counter fitted with a polyvinyl chloride window. The window was coated with a very thin layer of sputtered gold, and the total thickness of the window was approximately 200 $\mu g/cm^2$. The counter was filled with methane at a pressure of approximately 18 cm Hg.

The resolution (full width at half-maximum) of the spectrometer with our sources was 0.3% for kinetic energies above approximately 70 keV.

B. Energy Calibration

In order to minimize variations in the calibration of the double-focusing spectrometer, the magnet was demagnetized before each scan to a residual field of less than approximately 0.5 G and, during each scan, the magnet current was increased as nearly monotonically as possible. The primary energy calibration points were provided by conversion lines from transitions in Ir^{188} and Os^{188}, daughter nuclides of Pt^{188} which was present in the sources. The kinetic energies of conversion lines accompanying transitions in these nuclides have been measured to high precision with the iron-free, double-focusing spectrometer at the Chalk River Laboratory.[14] A list of the conversion lines which were used as primary calibration lines for the spectrometer

[13] R. L. Garwin, Rev. Sci. Instr. **29**, 223 (1958).

[14] R. L. Graham, J. S. Geiger, R. A. Naumann, and J. M. Prospero, Can. J. Phys. **40**, 296 (1962), and unpublished data by the same authors.

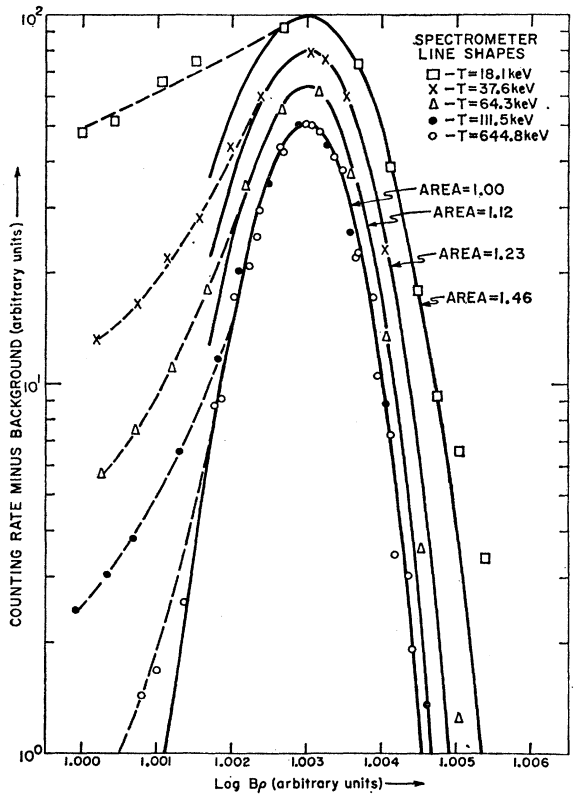

FIG. 5. Variation of the spectrometer line shape with energy. For comparison purposes the logarithm of the counting rate has been plotted versus logarithm of the magnetic rigidity for several energies. Note displacement of the peak positions for clarity of display.

is presented in Table II. Kinetic energy values were derived from the transition energies given in Table II and from the atomic binding energies given by Hill *et al.*[15] Each spectrometer scan was calibrated separately. The spectrometer readings corresponding to the peaks of the calibration lines in each scan were fitted by a weighted least squares method to a linear function of $B\rho$ (magnetic rigidity). The average percentage deviation of the $B\rho$ values for the calibration lines from the values predicted by the calibration curves is 0.025%; the maximum value is 0.080%.

Similar calibration procedures were used for spectra obtained with the permanent magnet spectrographs.

C. Identification of Lines

Spectra were first recorded with the permanent magnet spectrographs and a preliminary classification of lines according to nuclide was made. Thereafter, measurements on two sources were made with the double-focusing spectrometer, in order to obtain better information on the intensities and half-lives of the individual lines and to make a partial search for lines

[15] R. D. Hill, E. L. Church, and J. W. Mihelich, Rev. Sci. Instr. 23, 523 (1952).

TABLE II. Primary calibration lines.

Nuclide	Transition energy (keV)	Lines used
Ir^{188}	41.94±0.05	L_I, M_I
Ir^{188}	54.76±0.05	L_{II}, L_{III}
Ir^{188}	98.38±0.05	K
Ir^{188}	140.31±0.05	K, L_I
Ir^{188}	187.64±0.05	K, L_I
Ir^{188}	195.13±0.05	K, L_I
Os^{188}	155.03±0.03	L_{III}
Os^{188}	322.91±0.04	K
Os^{188}	478.07±0.04	K
Os^{188}	633.07±0.05	K

not seen on the plates. The work of Harmatz *et al.* on transitions in Ir^{189}, Ir^{191}, and Os^{189},[3] the work of Graham *et al.* on transitions in Os^{188}, and an unpublished study of transitions in[14] Ir^{188} were particularly helpful in our analysis of the spectrometer data.

The observed lines were first classified on the basis of energy according to their possible assignment to known transitions. Because of the multiplicity of transitions, there were many lines which could be assigned to more than one transition on this basis. Also, many of the observed lines were unresolved or poorly resolved mixtures of single lines. In many cases it was possible to clarify ambiguous assignments and to determine the energies and intensities of the component parts of composite lines by supplementing the energy classification with analyses of the decay of many line intensities as a function of time, and with the use of the experimentally determined line shape to decompose composite lines into their components. The half-lives used in performing the decay analyses were those determined in this work for Pt^{189} and Ir^{189}, and the published values for the remaining nuclides.

A knowledge of the spectrometer line shape, a graph of the logarithm of (counting rate minus background counting rate) versus the logarithm of $B\rho$, was essential for determining the energies and intensities of component parts of composite lines. The variation of this line shape with energy is illustrated in Fig. 5. The inner solid curve, which closely approximates the points for an electron line at 644.8 keV, represents the line shape in the limit of high energy. The remaining solid curves are derived from the inner solid curve by a change of scale along the abscissa. For purposes of clarity, the curves which correspond to different energies are displaced vertically in the figure. The dashed lines indicate deviations of the observed line shapes from the solid curves. If the functions represented by the solid curves are normalized to the same peak height and graphed with counting rate as ordinate and logarithm of $B\rho$ as abscissa, then the relative areas under the curves so obtained are the areas indicated in Fig. 5. A graph of these relative areas as a function of energy provides a correction curve for converting peak heights to intensities. The reported electron line intensities were

TABLE III. Multipole assignments and intensities for transitions in Ir^{189}.

Transition energy (keV)	Gamma intensity	Multipole assignment[a]	Transition intensity[b]	
71.62±0.06	···	$M2$	55	(from L_{I} and L_{III} electron intensities)
82.06±0.15	···	probably $E1$, $M1$, $M2$, or $M3$	···	
94.24±0.07	120	$E2$	750	
113.82±0.10	61	$M1+E2(5\lesssim\delta^2\lesssim 10)$	365	
141.06±0.06	124	$M1$	400	
176.3 ±0.3	···	···	···	
181.33±0.15	···	···	···	
186.7 ±0.2	137	$E2$	190	
(189.0)	···	···	···	
190.8	···	···	···	
203.7 ±0.4	···	···	···	
223.33±0.18	···	···	···	
225.6 ±0.2	···	···	···	
243.4 ±0.2	100	$E2$	116	
252.0 ±0.5	···	···	···	
258.2 ±0.2	···	$E2$ or $E3$	42($E2$) or 6($E3$)	(from L_{II} and L_{III} electron intensities)
300.4 ±0.2	54	$E2$	60	
317.6 ±0.2	42	$M1$	50	
403.8 ±0.5	32	$E2+M1(\delta^2\approx 0.4)$	35	
542.3 ±0.8	···	···	···	
544.8 ±0.4	134	$E2+M1(\delta^2\approx 0.6)$	140	
568.8 ±0.4	98	$M1+E2(\delta^2\approx 2.2)$	100	
607.2 ±0.7	114	$M1+E2(\delta^2\approx 3)$	120	
626.9 ±0.4	71	$E2$	70	
644.1 ±0.6	···	···	···	
720.9 ±0.5	156	$E2+M1(\delta^2\approx 0.56)$	160	
735.5 ±0.7	···	···	···	
792.4 ±0.7 / 798.1 ±1.5	27	···	···	

[a] Multipole assignments are based on comparison of experimental and theoretical K- and L-shell conversion coefficients and ratios.
[b] Unless otherwise specified transition intensities are calculated from the gamma intensities and theoretical K- and L-shell conversion coefficients.

obtained by multiplying peak heights (with background subtracted) by the appropriate relative areas.

V. RESULTS AND DISCUSSION

In Table III we present the transition energies, relative gamma intensities, multipole assignments, and relative transition intensities for proposed levels in Ir^{189}. The theoretical internal-conversion coefficients which were used in determining multipole assignments and transition intensities were interpolated from the compilations of Sliv and Band[16]; the compilation of Rose[17] was used as a check. In Table IV, transition energies, electron line intensities, and experimental conversion coefficients are given. Where a mixture of two or more lines is indicated, the quoted intensity is computed from the peak height of the composite line. Except for the transitions at 189.0 and 190.8 keV, the transition energies are based on energy measurements with the double-focusing spectrometer. The transition energies are determined from the observed kinetic energies of selected lines. The stated uncertainties in the energies have the approximate meaning of probable errors; they are derived from the degree of accuracy of the calibration and from the precision with which the magnet settings corresponding to the peaks of the pertinent conversion lines could be determined. The stated uncertainties in the electron intensities are nearer maximum errors than probable errors. For transitions whose multipolarities could be determined primarily by L subshell intensities and whose K lines are below ~100 keV, the quoted intensities of the K lines are always lower than is predicted by the theoretical conversion coefficients. This discrepancy becomes larger for lower values of the K kinetic energy. Thus, it is to be assumed that the tabulated intensities of all lines with kinetic energies below ~100 keV are systematically too low.

Multipolarity assignments for most transitions were made on the basis of the best agreement of electron line intensity ratios with the ratios of the theoretical conversion coefficients. The experimental conversion coefficients listed in Table IV were calculated from conversion electron line intensities and gamma ray intensities on the assumption that the 243.4 keV transition is pure $E2$. This assumption is firmly substantiated by a comparison of the experimental electron line intensity ratios with the theoretical K- and L-shell conversion coefficient ratios for this transition. Of the theoretical conversion coefficient ratios for the first five electric and magnetic multipoles—$E1$, ···, $E5$, and

[16] L. A. Sliv and I. M. Band, Academy of Sciences, USSR, 1956 and 1958 (unpublished) (English transl. issued by Physics Department, University of Illinois, Urbana, Illinois as Reports Nos. 57 ICCK1 and 58 ICCL1) (unpublished).
[17] M. E. Rose, *Internal Conversion Coefficients* (Interscience Publishers, Inc., New York, 1958).

TABLE IV. Conversion electron data for transitions in Ir^{189}.

Transition energy (keV)	Shell	Electron intensity[a,b]	Conversion coefficient (experimental)	Comments
71.62±0.06	L_I	(8.0±0.8)×10²(*A*)	···	
	L_{II}	(8.6±3.9)×10¹(*A*,*C*)	···	
	L_{III}	(3.0±0.7)×10²	···	
	$M_{I,II}$	(7.2±2.9)×10²	···	Probable admixture of Ir^{189} 82.06 L_I.
82.06±0.15	L_I	(6.9±2.8)×10²	···	Probable admixture of Ir^{189} 71.62 $M_{I,II}$.
	L_{II}	≲1.3×10³	···	Unresolved line.
	L_{III}	≲5.2×10²	···	Unresolved line.
	M_{III}	(2.4±2.1)×10²(*D*)	···	Weak evidence. Intensity deduced from anomalous decay of Ir^{191} 82.45 M_{II}.
94.24±0.07	*K*	(2.8±0.8)×10²	0.12	
	L_I	≲7.5×10²	≲0.32	Unresolved line.
	L_{II}	(2.4±0.5)×10³(*B*)	1.0	
	L_{III}	(2.1±0.3)×10³(*D*)	0.90	
	$M_{II,III}$	(9.3±1.8)×10²	0.40	
113.82±0.10	*K*	(1.1±0.1)×10³	0.93	
	L_I	(5.0±1.0)×10²	0.42	Probable admixture of Ir^{189} 176.3 *K*.
	L_{II}	(1.5±0.5)×10²	0.13	
	L_{III}	(1.4±0.5)×10²	0.12	
	$M_{I,II}$	(3.6±1.1)×10²		Probable admixture of Ir^{189} 186.71 *K*.
141.06±0.06	*K*	(1.7±0.2)×10³	0.71	
	L_I	(3.5±0.4)×10²	0.15	Probable admixture of Ir^{189} 203.7 *K*.
	L_{II}	≲4.7×10¹	≲0.02	Unresolved line.
	N	(1.6±0.7)×10¹	0.007	
176.3 ±0.3	*K*	(5.0±1.0)×10²		Probable admixture of Ir^{189} 113.82 L_I.
	$L_{I,II}$	(2.9±0.6)×10¹		
	L_{III}			Obscured.
181.33±0.15	*K*	(7 ±3)×10¹		
186.7 ±0.2	*K*	(3.7±0.8)×10²	0.14	Probable admixture of Ir^{189} 113.82 M_I.
	L_I	(1.1±0.5)×10²	0.041	
	L_{II}	≲5.4×10¹	≲0.020	
	L_{III}	(1.1±0.4)×10¹		Probable admixture of Ir^{189} 252.0 *K* and Ir^{189} 189.0 $L_{I,II}$.
(189.0)	*K*	[40]		Seen on photographic plates. Could be Ir^{189} 113.82 *N*.
	$L_{I,II}$	(1.1±0.4)×10¹		Probable admixture of Ir^{189} 252.0 *K* and Ir^{189} 186.7 L_{III}.
190.8	*K*	[40]		Seen on photographic plates. Quoted energy is average of this work and that of Harmatz *et al.*
203.7 ±0.4	*K*	(3.5±0.5)×10²		Probable admixture of Ir^{189} 141.06 L_I.
	L_I	[80]		Seen on photographic plates.
223.33±0.18	*K*	(7 ±4)×10¹		
	L_{II}	(2.5±0.9)×10¹		Probable admixture of Ir^{191} 223.7 L_I, 221.9 L_{III}, and 213.8 *M*.
	L_{III}	(1.2±0.6)×10¹		Probable admixture of Ir^{189} 225.6 L_I.
225.6 ±0.2	*K*	(2.5±2.0)×10¹		
	L_I	(1.2±0.6)×10¹		Probable admixture of Ir^{189} 223.33 L_{III}.
243.4 ±0.2	*K*	(1.6±0.2)×10²	0.082	See text.
	$L_{I,II}$	(7.5±2.0)×10¹	0.039	L_I contribution ≲⅓ of L_{II} intensity. See text.
	L_{III}	(4.2±1.3)×10¹	0.022	See text.
	$M_{I,II}$	7.7±2.0	0.004	
	N	8.2±4.0	0.004	
252.0 ±0.5	*K*	(1.1±0.4)×10¹		Probable admixture of Ir^{189} 186.7 L_{III} and Ir^{189} 189.0 $L_{I,II}$.
	$L_{I,II}$	5.3±2.0		
258.2 ±0.2	*K*	≲5.9×10¹		
	L_I	≲2		
	L_{II}	(1.9±0.6)×10¹		
	L_{III}	9 ±3		
300.4 ±0.2	*K*	(5.4±0.8)×10¹	0.052	
	$L_{I,II}$	(1.8±0.4)×10¹	0.017	
	L_{III}	7.5±2.0	0.0072	
317.6 ±0.2	*K*	(1.4±0.1)×10²	0.17	
	$L_{I,II}$	(2.1±0.4)×10¹	0.026	
	L_{III}			Obscured.
	M	4.3±1.0	0.0053	
403.8 ±0.5	*K*	(3.3±0.6)×10¹	0.053	
	$L_{I,II}$	6 ±3	0.01	
542.3 ±0.8	*K*	≲2.3×10¹		Line reported by Harmatz *et al.*
	$L_{I,II}$	≲2.3×10¹		
	L_{III}	(8.0±1.0)×10¹		Probable admixture of Ir^{189} 607.2 *K* and Ir^{189} 544.8 $L_{I,II}$.
544.8 ±0.4	*K*	(7.3±0.7)×10¹	0.028	
	$L_{I,II}$	(8.0±1.0)×10¹	0.030	Probable admixture of Ir^{189} 607.2 *K* and Ir^{189} 542.3 L_{III}.

TABLE IV. (*continued*).

Transition energy (keV)	Shell	Electron intensity[a,b]	Conversion coefficient (experimental)	Comments
	L_{III}	$\lesssim 4$	$\lesssim 0.002$	
568.8 ±0.4	K	$(6.5\pm0.7)\times10^{1}$	0.035	
	$L_{I,II}$	11 ± 2	0.0058	
	L_{III}	$\lesssim 3$	$\lesssim 0.002$	
	M	3.6 ± 1.2	0.0019	
607.2 ±0.7	K	$(6.6\pm1.2)\times10^{1}$	0.030	Intensity computed assuming assigned multipolarity for Ir^{189} 544.8 and ignoring possible Ir^{189} 542.3 L_{III}.
	$L_{I,II}$	$(1.1\pm0.1)\times10^{1}$	0.0049	
	L_{III}	$\lesssim 1$	$\lesssim 0.0005$	
	M	2.9 ± 1.4	0.0013	
626.9 ±0.4	K	$(1.6\pm0.2)\times10^{1}$	0.012	
	$L_{I,II}$	3.3 ± 0.7	0.0024	
644.1 ±0.6	K	6.1 ± 1.0		Possible admixture of Ir^{189} 568.8 N.
720.9 ±0.5	K	$(4.4\pm0.3)\times10^{1}$	0.014	
	$L_{I,II}$	7.7 ± 1.5	0.0025	
	L_{III}	$\lesssim 2$	$\lesssim 0.0007$	
	$M+N$	2.7 ± 0.5	0.0009	
735.5 ±0.7	K	2.0 ± 0.5		
	$L_{I,II}$	1.6 ± 0.8		Probable admixture of Ir^{189} 798.1 K.
792.4 ±0.7	K	$6\ \pm2$		
	L	$\lesssim 0.5$		
798.1 ±1.5	K	1.6 ± 0.8		Probable admixture of Ir^{189} 735.5 $L_{I,II}$.

[a] Numbers in square brackets are estimates from photographic plates.
[b] A letter in parentheses following an intensity indicates that a contribution of different half-life has been subtracted. The origin of the subtracted contribution is designated by A-Auger electron, B-Os^{188}, C-Os^{189}, D-Ir^{191}.

$M1$, $\cdots$, $M5$—only the ratios for an $E2$ transition agree with the experimental values. The other theoretical ratios are in significant disagreement with the experimental values and, in particular, our data do not warrant inclusion of an $M1$ admixture. The experimental ratios are $K/(L_I+L_{II})/L_{III}=1/0.47/0.26$; $L_I/L_{II}\lesssim\frac{1}{3}$. (See Table IV for the experimental errors.) The theoretical values for an $E2$ transition are $K/(L_I+L_{II})/L_{III}=1/0.44/0.17$; $L_I/L_{II}=0.42$. For an $M1$ transition the values are $K/(L_I+L_{II})/L_{III}=1/0.165/0.00135$; $L_I/L_{II}=10.5$. For the computation of absolute conversion coefficients, based on the experimental gamma and electron line intensities, the relative gamma intensities which are given in Table III were renormalized so as to obtain the best fit of the computed conversion coefficients for the K and L_{III} lines of the 243.4-keV transition to the corresponding theoretical $E2$ coefficients. The conversion coefficients are presented in Table IV. These conversion coefficients were a very useful supplement to the electron line intensity ratios for assigning multipolarities to the transitions. In those cases in which there was sufficient experimental information to allow multipolarities to be independently deduced from the conversion coefficients and from the intensity ratios, the assignments deduced from the two methods agreed with one another. Mixing ratios have been calculated for $M1-E2$ mixtures and they are presented in Table III. The quantity δ^2 is defined as the ratio of the $M1$ gamma intensity to the $E2$ gamma intensity.

The half-life for the decay of Pt^{189} to Ir^{189} was measured by following the decay of the K line of the 113.82 keV transition in Ir^{189}. The value of the half-life, computed by a weighted least-squares method, is 10.87 ± 0.12 hours. The quoted uncertainty is the standard deviation. Evidence for decay quantitatively consistent with this half-life was obtained for the proposed transitions in Ir^{189} at 94.24, 113.82, 141.06, 181.33, 186.7, 223.33, 243.4, 252.0, 258.2, 317.6, 544.8, 568.8, 607.2, 626.9, 720.9, 735.5, and 792.4 keV. Evidence for decay with this half-life for the remaining transitions in Ir^{189} is more qualitative.

Evidence has been found for all but one of the transitions reported by Harmatz *et al.*; the energy values obtained by us are in reasonable agreement with theirs. No evidence for a transition at 802.0 keV was seen either with the permanent magnet spectrographs or the double-focusing spectrometer. In addition we have listed new transitions at 189.0, 252.0, and 798.1 keV. The existence of a transition at 798.1 keV was inferred because of difficulty in assigning a multipolarity to the 735.5-keV transition. If the 735.5 $L_{I,II}$ line were assumed to have no contribution from the proposed 798.1 K line, then the $L_{I,II}/K$ intensity ratio for the 735.5-keV transition excludes all multipole assignments except the unlikely $E4$, $E5$, or $M5$ multipoles. Even then, the agreement with the theoretical ratios would be poor. The decay of the $L_{I,II}$ line of the 252.0 keV transition was observed to be consistent with the 10.87-hour half-life. The least certain of the newly proposed transitions is the one at 189 keV.

As an aid in constructing an energy level scheme for Ir^{189}, an IBM-7090 computer was used to seek combination relations among the measured transition

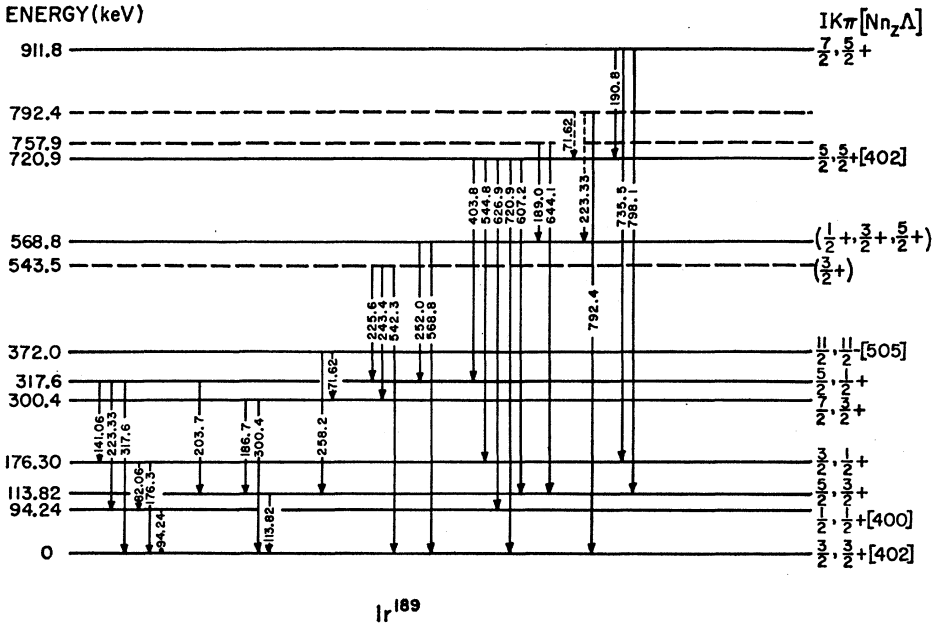

FIG. 6. Level scheme for Ir^{189}. New levels at 543.8, 568.8, 757.9, 792.4, and 911.8 keV are proposed. Dashed levels are less firmly established.

energies. The computer operated with the measured transition energies, E_i, and with the sets of sums of the energies, $E_{ij}=E_i+E_j$, $E_{ijk}=E_i+E_j+E_k$, and $E_{ijkl}=E_i+E_j+E_k+E_l$. The information obtained was pairs of numbers from these four sets which, to within a specified fractional error, were equal to one another. Specifically, equalities of the following types were considered: $E_i=E_{jk}$, $E_i=E_{jkl}$, $E_i=E_{jklm}$, $E_{ij}=E_{kl}$, $E_{ij}=E_{klm}$, and $E_{ijk}=E_{lmn}$. The latter two types of equalities were not particularly useful because of the very large number of accidental equalities which may be expected.

The energy level diagram which we have constructed is shown in Fig. 6. All of the 29 reported transitions, except the one at 181.33 keV, are included in the level scheme. The sum relations implied by the diagram are accurate to within 0.15%, except for the case of the observed 542.3-keV transition which is assigned as the ground state transition from the 543.5-keV level. Of the twelve excited states indicated, seven are included in the decay scheme of Harmatz *et al.* Of the five additional levels, those at 568.8 and 911.8 keV are regarded as fairly certain, whereas those at 543.5, 757.9, and 792.4 keV are regarded as tentative. The two cascade transitions, at 71.62 and 223.33 keV, which depopulate the 792.4-keV level are used elsewhere in the scheme. The spins and parities of that portion of the level diagram which was proposed by Harmatz *et al.* are in agreement with the transition multipolarities which we have observed and these assignments are included in Fig. 6.

The spin and parity assignment of the level at 568.8 keV is $\frac{1}{2}+$, $\frac{3}{2}+$, or $\frac{5}{2}+$ based on the $M1+E2$ assignment to the ground-state transition.

The level at 911.8 keV may be the $\frac{7}{2}+$ member of the $K=\frac{5}{2}$ rotational band which is based on the level at 720.9 keV. The competition of the 190.8-keV transition, leading to the $\frac{5}{2}+$ member of the $K=\frac{5}{2}$ band, with the 735.5-keV transition, leading to the $\frac{3}{2}+$ member of the $K=\frac{1}{2}$ band, and with the 798.1-keV transition, leading to the $\frac{5}{2}+$ member of the $K=\frac{3}{2}$ band, could support this interpretation. Further support for the $\frac{7}{2}+$ assignment is provided by the similarity in energy between the 190.8-keV and 186.7-keV transitions, the latter being firmly established as the $\frac{7}{2}+\rightarrow\frac{5}{2}+$ transition in the $K=\frac{3}{2}$ band.

The level at 543.5 keV is partly depopulated by the pure $E2$ transition at 243.4 keV, leading to the $\frac{7}{2}+$ member of the $K=\frac{3}{2}$ band. A likely spin and parity assignment for that level is $\frac{3}{2}+$. No spin and parity assignments can be proposed for the levels at 757.9 and 792.4 keV on the basis of the available information.

ACKNOWLEDGMENTS

We wish to express our thanks to W. Goodell and his staff of the Nevis cyclotron for performing the proton bombardments of our iridium targets. Our gratitude to those who assisted in taking and analyzing data is especially extended to J. P. Boris, for his very competent work in writing computer programs, and to A. D. Jackson, for his excellent assistance in analyzing photographic plates taken with the permanent magnet spectrographs.